ELSEVIER

Journal of Molecular Catalysis A: Chemical 163 (2000) 55–65

JOURNAL OF MOLECULAR CATALYSIS A: CHEMICAL

www.elsevier.com/locate/molcata

Supported metal cluster catalysts

B.C. Gates*

Department of Chemical Engineering and Materials Science, University of California, Davis, CA 95616, USA

Received 8 March 2000; accepted 30 June 2000

Abstract

Highly dispersed metal catalysts containing supported clusters of only several metal atoms each, exemplified by Ir_4 and Ir_6, were prepared by removal of CO ligands from supported precursors, for example, $[Ir_4(CO)_{12}]$ and $[Ir_6(CO)_{16}]$. Transmission electron microscopy (TEM), extended X-ray absorption fine structure spectroscopy and density functional theory indicate the metal–support-oxygen coordination numbers and distances, which identify the supports as multidentate oxygen-donor ligands. Theory indicates that Ir_4 clusters in zeolite NaX are neutral or slightly negatively charged and that cluster-support bonding induces a polarization of the cluster that could affect reactivity and catalysis. Supported catalysts prepared from precursors with noble metal-oxophilic metal bonds are modeled as clusters of a few atoms of the noble metal 'nested' in a supported cluster of the oxophilic metal oxide, which helps to anchor and stabilize the noble metal clusters. Changes in the oxide support have only modest effects on the catalytic activities of supported metal clusters for toluene hydrogenation, but the catalytic activity of γ-Al_2O_3-supported Ir clusters per exposed Ir atom increases with increasing cluster size, and this observation remains to be explained. © 2000 Published by Elsevier Science B.V.

Keywords: Catalysts; Metal clusters; Transmission electron microscopy

1. Introduction

In his 1985 essay 'Heterogeneous Catalysis by Metals,' Boudart [1] classified supported metals according to the average metal particle size and emphasized the importance of investigating the smallest particles, those with diameters less than 1 nm, which we call clusters. In his conclusion, Boudart wrote,

> . . . The largely unexplored domain involving particle sizes *below* 1 nm appears the most challenging for the future in terms of preparation, characterization and potential enhancement of reactivity [2]. Moreover, *here the domain of heterogeneous catalysis rejoins the domain of homogeneous catalysis* or that of heterogeneous catalysis by free or immobilized organometallic metal cluster complexes [3]. Finally, in this size range metal-support interactions are expected to be particularly important. Much remains to be done to understand the nature of these interactions [4]. [1]

The goal of the following account is to supplement Boudart's with a summary of developments in the understanding of supported metal clusters.

2. Supported metal clusters in practical catalysts

Using H_2 chemisorption to probe the reactive metal surfaces in supported metals, Spenadel and Boudart [5] in 1960 inferred that particles averaging <1 nm in diameter were present in Pt/η-Al_2O_3. Researchers

* Tel.: +1-530-752-3953; fax: +1-530-752-1031.

[1] Reference numbers were changed in the quotation to correspond to the numbering in this paper.

1381-1169/00/$ – see front matter © 2000 Published by Elsevier Science B.V.
PII: S1381-1169(00)00399-X

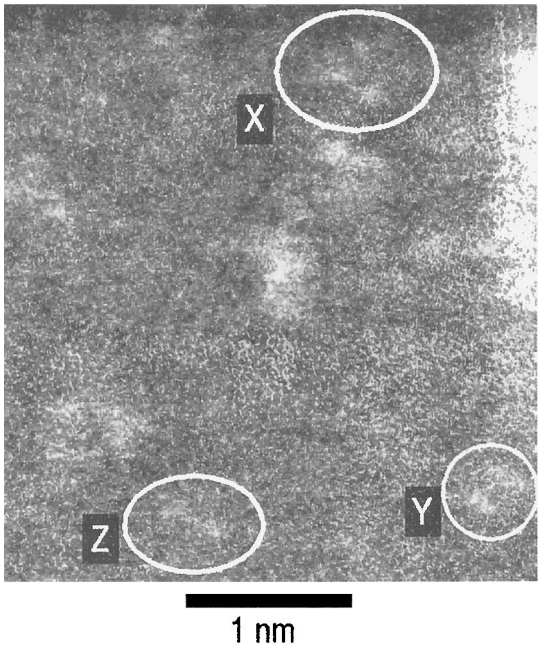

Fig. 1. Scanning transmission electron microscopy image of Pt clusters supported on γ-Al_2O_3 [6]. The region marked X indicates a Pt_3 cluster and those marked Y and Z indicate Pt_2 clusters.

long suspected that even smaller clusters existed in naphtha reforming catalysts, and now there are confirming images of clusters of two and three atoms in Pt/γ-Al_2O_3 obtained by scanning transmission electron microscopy [6] (Fig. 1). Pt clusters with as few as about 5–12 atoms each, on average [7,8], supported on zeolite LTL have been imaged with high-resolution transmission electron microscopy (TEM) (Fig. 2). Well-prepared catalysts of this type, used industrially for selective naphtha reforming to make aromatics, incorporate Pt almost exclusively in the form of such small clusters, largely inside the zeolite pores.

3. Preparation

These supported Pt catalysts were made, for example, by impregnation with a platinum ammine salt, calcination and reduction in H_2. The metal clusters and particles are nonuniform in size and shape, as is typical of industrial catalysts. To understand supported metal clusters better, researchers have worked to prepare them with nearly unique sizes, as follows.

3.1. Impingement of a beam of size-selected gas-phase clusters

This method, investigated primarily by physicists [9–12], has the advantage that, in prospect, it can be used with any metal of any cluster size. Disadvantages are the restriction to planar supports and the uncertainty of the cluster size distributions after deposition. Heiz et al. [11,12] asserted that ‘soft landings’ give uniform supported clusters, but no experimental results yet confirm the assertion.

3.2. Adsorption of metal carbonyl clusters followed by decarbonylation

The goal is to form metal carbonyls (e.g. $[Ir_4(CO)_{12}]$) molecularly dispersed on a support and to remove the CO ligands without disrupting the metal frame. Advantages of this method are its applicability to many porous oxide supports and the opportunities to track the chemistry of chemisorption and decarbonylation. A disadvantage is the probable restriction to a few metals (e.g. Ru, Rh, Ir, Os). Furthermore, when the metal carbonyl cluster precursor is synthesized on the support and not simply adsorbed from solution, the best yields yet reported are only about 80–90%, as determined by ^{13}C NMR spectroscopy [13,14] — the impurity species are most likely mononuclear metal complexes and metal clusters similar in size to those desired. The decarbonylation is not simple desorption of CO but instead involves reaction of CO with support groups such as OH and likely involves breaking of C–O bonds and may leave ligands such as C on the decarbonylated clusters [15].

3.3. Ship-in-a-bottle synthesis of metal carbonyl clusters followed by decarbonylation

When the pores of the support (e.g. zeolite X) are too narrow to allow entry of the precursor metal carbonyl cluster (e.g. $[Ir_4(CO)_{12}]$), simple adsorption in the pores is precluded and, instead, a ship-in-a-bottle synthesis is carried out with precursor molecules (e.g. $[Ir(CO)_2(acac)]$, acac is acetylacetonate) small enough

Fig. 2. Transmission electron microscopy image of Pt clusters supported in zeolite LTL [7].

to pass through the apertures into the supercages where they self-assemble in the presence of CO to form metal carbonyl clusters (e.g. $[Ir_4(CO)_{12}]$) trapped because they are too large to fit through the apertures [16,17]. The resultant encaged metal carbonyl cluster is determined by the relative stabilities of the candidates and by the geometric constraints of the cage; for example, $[HIr_4(CO)_{11}]^-$ and, from it, $[Ir_6(CO)_{15}]^{2-}$ form in zeolite NaX supercages, but $[Ir_8(CO)_{15}]^{2-}$ clusters are too large to fit in the cages and do not form [18].

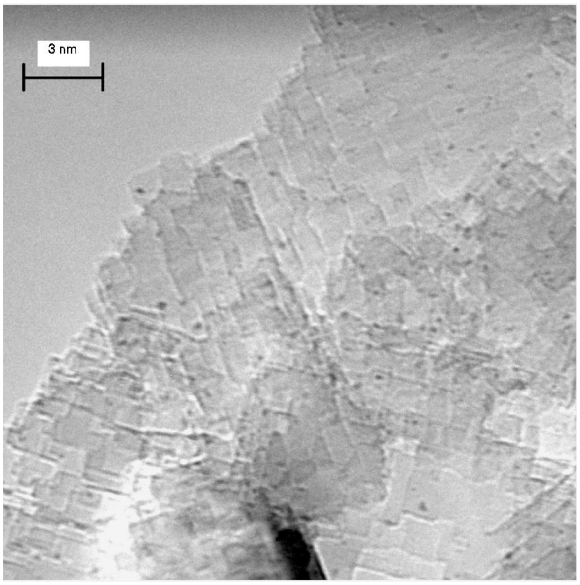

Fig. 3. Transmission electron microscopy image of Os_5C clusters supported on MgO [14].

4. Cluster sizes and shapes

High-resolution TEM (Fig. 3) shows clusters made by decarbonylation of $[Os_5C(CO)_{14}]^{2-}$ on MgO. These are all approximately 0.6 nm in diameter, consistent with EXAFS data and the dimensions of the metal frame of $[Os_5C(CO)_{14}]^{2-}$. EXAFS spectroscopy accurately characterizes the geometries of cluster frames, as illustrated by a comparison of EXAFS parameters for $[Rh_6(CO)_{16}]$ dispersed molecularly in a zeolite and XRD parameters for $[Rh_6(CO)_{16}]$ in the crystalline state (Table 1). These data are in good agreement with each other, so that one has confidence in EXAFS spectroscopy for determining geometries of metal cluster frames, decarbonylated or not — provided that they are not much larger than 5-atom or 6-atom clusters and have simple, regular shapes; data summarized elsewhere bolster this statement [23]. Numerous EXAFS data are consistent with supported tetrahedral (Ir_4) and octahedral (Ir_6 and Rh_6) clusters, made respectively from supported metal carbonyls with tetrahedral and octahedral metal skeletons [23–25].

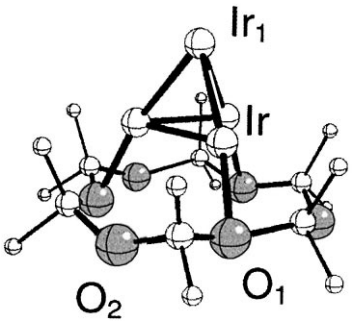

Fig. 4. Ir_4 cluster supported at the six-ring of zeolite NaX [26].

Density functional theory confirms the stability of Ir_4 in zeolite NaX (with the interaction assumed to occur at the six-ring facing a supercage [26]) (Fig. 4). It also confirms the stability of Os_5C supported on the

Table 1
Structural parameters determined by XRD for $[Rh_6(CO)_{16}]$ in the crystalline state and by EXAFS spectroscopy for $[Rh_6(CO)_{16}]$ dispersed in zeolite NaY[a]

XRD parameters [19]						EXAFS parameters						References
Rh–Rh		Rh–C		Rh–O*		Rh–Rh		Rh–C		Rh–O*		
N	*R* (nm)	*N*	*R* (nm)	*N*	*R* (nm)	*N*	*R* (nm)	*N*	*R* (nm)	*N*	*R* (nm)	
4.0	0.278	2.0	0.186[b]	4.0	0.306	4.0	0.276	2.1	0.187[b]	–	–	[20,22]
		2.0	0.217[c]					2.0	0.217[c]			
						4.0	0.276	2.1	0.193[b]	4.1	0.299	[21]
								2.2	0.227[c]			
						4.1	0.277	2.4	0.187[b]	2.6	0.282[b]	[22]
								3.2	0.218[c]	3.5	0.296[c]	

[a] Notation: *N*, coordination number for shell; *R*, average shell radial distance; O*, carbonyl oxygen.
[b] Terminal carbonyl ligand.
[c] Bridging carbonyl ligand.

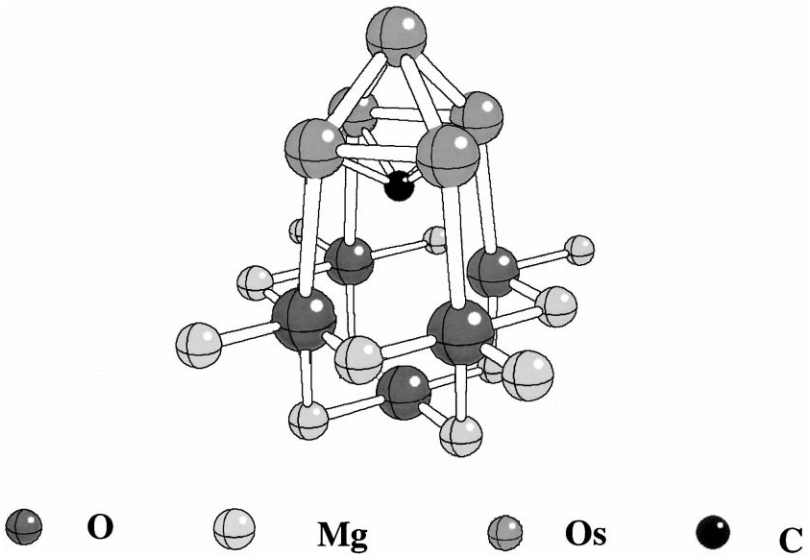

Fig. 5. Os_5C supported on MgO, as modeled by density functional theory [27].

(1 0 0) face of MgO at V_s defect sites (where Mg ions are missing, Fig. 5) but not on the defect-free (1 0 0) face [27].

5. Supports as ligands

EXAFS spectroscopy characterizes the metal-support interface in terms of M–O coordination numbers and distances, but the uncertainty in the parameters is markedly greater than for first-shell metal–metal contributions. Both relatively short metal-support oxygen ($M–O_s$) distances of about 0.21–0.22 nm and relatively long $M–O_s$ distances of about 0.25–0.27 nm are typical EXAFS results [28], being determined with precisions of 1–2%. The $M–O_s$ coordination numbers are must less precise than the distances and do not lead to strong generalizations, save that a $M–O_s$ coordination number of roughly 1–2 is typical of noble metal clusters on oxide and zeolite supports.

More reliable evidence of metal-support interactions has been obtained from EXAFS data characterizing supported mononuclear metal complexes, exemplified by carbonyls of the oxophilic metal Re [29]. Metal carbonyls with terminal CO ligands yield well to EXAFS analysis because the technique distinguishes metal-low-Z backscatterer contributions from metal–CO contributions as a consequence of the multiple scattering in the linear M–C–O moiety.

Rhenium carbonyl complexes on MgO are regarded as prototypes, having been synthesized from various precursors {$[HRe(CO)_5]$, $[DRe(CO)_5]$, $[Re_2(CO)_{10}]$ and $[H_3Re_3(CO)_{12}]$} on MgO powder [29–32] and on ultrathin MgO films (on single-crystal Mo) exposing the (1 1 1) face [33]. EXAFS data confirm approximately three CO ligands per Re atom and approximately three support oxygen atoms neighboring each Re atom, consistent with infrared spectra demonstrating the symmetry [30–33]. Two limiting-case structures are indicated (Fig. 6) [34].

The average rhenium tricarbonyl on a largely dehydroxylated MgO powder was found to have

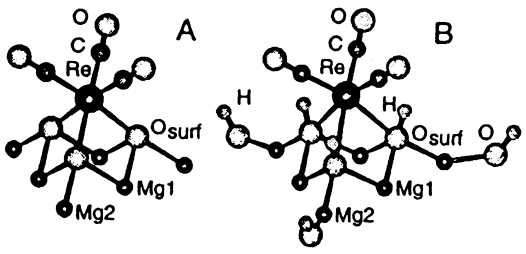

Fig. 6. Structures of rhenium carbonyls bonded to MgO modeled with density functional theory [34].

Table 2
Calculated properties of $Re(CO)_3\{OMg\}_3$ and $Re(CO)_3\{HOMg\}_3$ compared with experimental results[a]

Structure	r(Re–O)	r(Re–C)	r(C–O)	r(O–Mg1)	r(O–Mg2)	E_b	ν(Re–MgO)	ν(Re–CO)
$Re(CO)_3\{OMg\}_3$								
$Re(0)(CO)_3/V_s^-$	0.226	0.190	0.118	0.203	0.202	2.79	528	510
$Re(I)(CO)_3/V_s^-$ [b]	0.215	0.195	0.116	0.204	0.209	3.51	552	479
$Re(I)(CO)_3/V_s$	0.205	0.202	0.115	0.205	0.215	2.74	551	439
Experiment[c]	0.215	0.188						
$Re_3(CO)_3\{HOMg\}_3$								
$Re(I)(CO)_3/V_s(OH)$	0.255	0.191	0.117	0.203	0.207	0.67	417	523

[a] Distances r in nm, binding energy E_b of $Re(CO)_3$ species to MgO in eV per Re–O bond (three bonds), vibrational frequencies ν in cm^{-1}; V_s refers to surface defect site (see text). Refer to Fig. 6 for structures of $Re(CO)_3\{OMg\}_3$ and $Re(CO)_3\{HOMg\}_3$, Mg atoms are numbered in this figure.

[b] Also represents $Re(0)(CO)_3/V_s$ where $E_b = 3.37$ eV per Re–O bond with respect to $Re(CO)_3$ and $\{OMg\}_3(V_s)$.

[c] Experimental distances from EXAFS spectroscopy for structure approximated as $Re_3(CO)_3\{OMg\}_2\{HOMg\}$ [29,30].

approximately two oxygen ligands of the support and one OH ligand of the support [30]. Structural data representing, on average, $Re(CO)_3\{OMg\}_3$ and $Re(CO)_3\{HOMg\}_3$ (where the braces refer to groups terminating the support) are summarized in Table 2. Density functional theory gave structure parameters for $Re(CO)_3\{OMg\}_3$ bonded at a corner site of MgO (consistent with the observed symmetry), in good agreement with the data for the experimental sample represented as approximately $Re(CO)_3\{OMg\}_2\{HOMg\}$ (Table 2).

The Re–Os distance of 0.215 ± 0.003 nm determined by EXAFS spectroscopy agrees well with the theoretical value of 0.215 nm for $Re(CO)_3\{OMg\}_3$ (Fig. 6, Table 2). The supported complexes are formally coordinatively saturated (18-electron) and the Re-backscatterer distances and symmetries indicate that they are close analogues of molecular organometallic compounds [34]. The theoretical results show that the Re–O_s bond energy in $Re(CO)_3\{OMg\}_3$ (3.5 eV) is greater than the Re–CO bond energy (2.4–2.5 eV), confirming the role of the oxide support as a strongly bonded (tridentate) ligand [34] and demonstrating the appropriateness of representing the surface complexes as analogues of molecular species. Results such as these suggest that support effects in catalysis may be regarded as ligand effects, this suggestion links surface catalysis and molecular (homogeneous) catalysis.

As experimental results characterizing M–O_s contributions in supported metal clusters are less informative than those characterizing such contributions in supported mononuclear metal complexes, density functional theory has been used to understand the cluster-support interface better [26,27]. The parameters characterizing Ir_4 in zeolite NaX (Fig. 4) indicate Ir–O distances of about 0.22 nm, in good agreement with EXAFS data [26]. When the structure of Fig. 4 is rotated 60°, the theory indicates an Ir–O distance of about 0.27 nm, in agreement with the longer distances observed by EXAFS spectroscopy (but this agreement may be fortuitous). Similarly, theoretical results for Os_5C on MgO (Fig. 5) indicate Os–O_s distances of about 0.21 nm, in good agreement with the EXAFS data, and when the structure is rotated 90°, the distance is about 0.26 nm, again in good agreement with EXAFS data for the longer Os–Os distance [14,28] (but this agreement may also be fortuitous).

6. Cages as supports

Some early attempts to prepare supported metals as extremely small clusters were based on the idea that zeolite cages could limit the sizes of the clusters and provide resistance to migration and aggregation. Samant and Boudart [35] assessed the literature in 1991 and concluded that various characterization techniques gave different estimates of the average cluster size. The inconsistencies may be related both to nonuniformities of the clusters and limitations of the techniques. More nearly uniform samples include Ir_4, Ir_6 and Rh_6 in zeolite NaY and their precursors, $[Ir_4(CO)_{12}]$, $[Ir_6(CO)_{16}]$ and $[Rh_6(CO)_{16}]$ in the zeolite, characterized by EXAFS spectroscopy

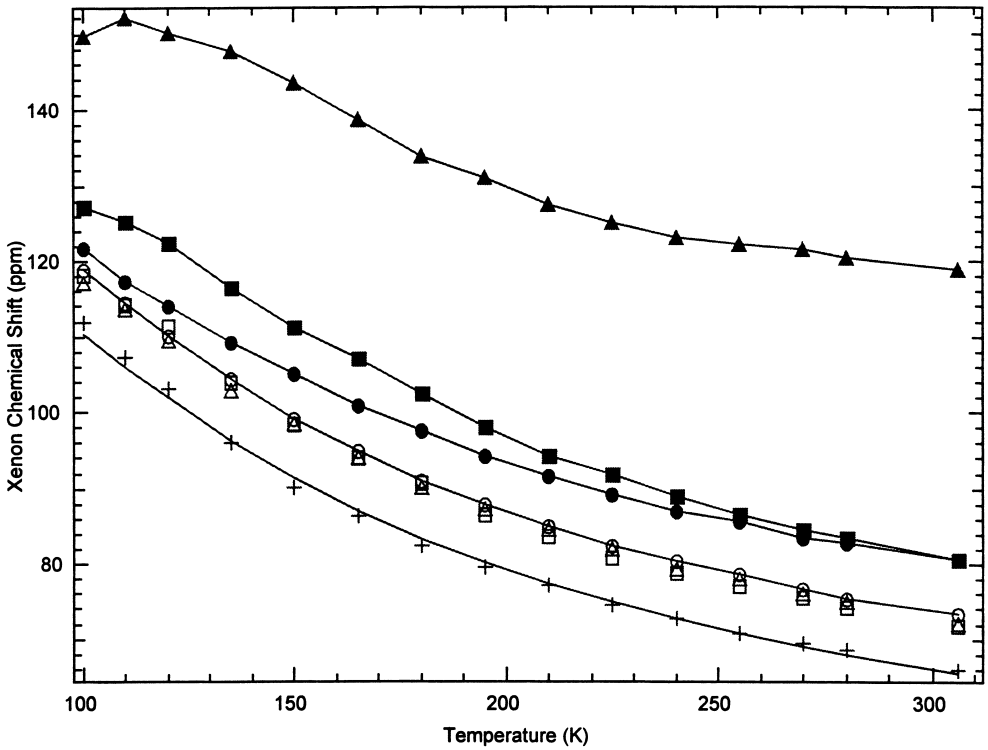

Fig. 7. ^{129}Xe NMR chemical shifts characterizing xenon in (+) zeolite NaY and in zeolite NaY containing clusters modeled as (▲) $[Ir_4(CO)_{12}]$, (■) $[Ir_6(CO)_{16}]$, (●) $[Rh_6(CO)_{16}]$, (△) Ir_4, (□) Ir_6 and (○) Rh_6 [36].

[24,26]. Further characterization of these encaged clusters with ^{129}Xe NMR spectroscopy over a wide temperature range (Fig. 7) led to the recognition that the Xe atom–metal interactions are weak and almost the same for each decarbonylated metal cluster; in contrast, the interactions of Xe atoms with the metal carbonyl clusters are strong, and the chemical shift for Xe in the zeolite containing $[Ir_4(CO)_{12}]$ was found to be markedly greater than that for Xe in the zeolite containing $[Ir_6(CO)_{16}]$ or $[Rh_6(CO)_{16}]$ (Fig. 7), suggesting that Xe atoms were excluded from the cages containing either of the latter two clusters because there was too little space for both the cluster and the Xe atom [36]. In contrast, a Xe atom just fits in a cage with the smaller $[Ir_4(CO)_{12}]$, leading to a significant interaction. These results illustrate an advantage of samples with nearly monodisperse clusters and suggest the need for more work to determine how (or whether) the sizes of encaged metal clusters may be estimated from Xe chemical shifts.

7. Site-isolated nanosupports

When a supported metal on an oxide is prepared from an adsorbed precursor incorporating a noble metal bonded to an oxophilic metal, the result may be small noble metal clusters, each more or less nested in a cluster of atoms of the oxophilic metal which is oxidized and anchored through metal–oxygen bonds to the support [37]. The simplest such structure appears to be Re_4Pt_2 made from $[Re_2Pt(CO)_{12}]$; EXAFS data led to the postulate of a surface species in which Re strongly interacts with the oxygen atoms of the support and also with Pt (Fig. 8) [38]. When one of the metals in a supported bimetallic cluster is noble and the other oxophilic, the oxophilic metal interacts more strongly with the support than the noble metal; if the bimetallic frame of the precursor is kept (nearly) intact, then this metal-support interaction helps keep the noble metal highly dispersed. Other examples of such ‘nested’ noble metal clusters have been made from the follow-

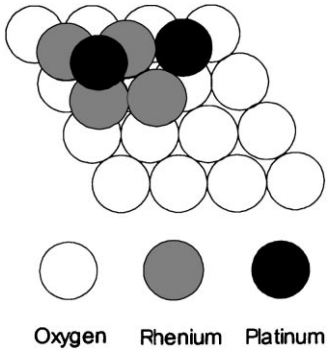

Fig. 8. Structural model of Re_4Pt_2 clusters supported on γ-Al_2O_3 [38].

ing precursors: $[Pd_2Mo_2(CO)_6(C_5H_5)_2(PPh_3)]$ [37], $[PtMo_2(CO)_6(C_5H_5)_2(PhCN)_2]$ [39], $[PtW_2(CO)_6(C_5H_5)_2(PhCN)_2]$[40], $[Pt_2W_2(CO)_6(C_5H_5)_2(PPh_3)_2]$ [41] and $[Ru_{12}C_2Cu_4Cl_2(CO)_{32}][PPN]_2$ [42]. Pt clusters of as few as four atoms, on average, are indicated by EXAFS data [41]. The Pt–W samples, for example, are quite stable, with the cluster size remaining essentially unchanged after oxidation–reduction cycles at 673 K [40,41]. The stability is attributed to the nanosupport (nest).

8. Metal–metal distances

The most accurate EXAFS parameters characterizing supported metal clusters are the metal–metal bond distances, which depend on the ligands. EXAFS spectroscopy and density functional theory were used to determine Ir–Ir distances in supported Ir_4 (Table 3); a comparison of EXAFS results for $[Ir_4(CO)_{12}]$ in the crystalline state with X-ray diffraction data indicates the reliability of the methods. The coordinatively saturated iridium carbonyl clusters all have Ir–Ir distances of nearly 0.271 nm, nearly matching the EXAFS values for supported Ir_4. In contrast, density functional theory shows that the Ir–Ir distance of free Ir_4 is about 0.02 nm less than this distance and that the Ir–Ir distance of Ir_4 at the six-ring of zeolite NaX (Fig. 4) is barely greater than the value representing the free cluster. The theory shows, however, that bonding of a single carbon ligand at a triangular face of the zeolite-supported cluster increases the Ir–Ir distance to a value close to the EXAFS value characterizing the supported Ir_4 [26]. This comparison strongly suggests that the supported clusters formed by decarbonylation of supported $[Ir_4(CO)_{12}]$ (or $[HIr_4(CO)_{11}]^-$) were not entirely free of ligands besides the support, it is plausible that C ligands formed from CO, for example, remained on the clusters.

EXAFS data characterizing supported Pt clusters or particles (nonuniform in size) showed an increase of 0.006 nm in the average Pt–Pt distance when an evacuated sample was brought in contact with H_2, the changes are reversible, and the average Pt cluster or particle size did not change as a result of the treatments [43]. These results are contrasted with those observed for supported Ir clusters. The Ir–Ir distance is apparently a less sensitive indicator of the ligand environment of a cluster than the Pt–Pt distance. Thus,

Table 3
Ir–Ir distances in tetrairidium clusters and bulk Ir metal[a]

Structure	Ir–Ir distance (nm)	Method of determination of structure and distance
Free Ir_4	0.2436	DFT
Bulk Ir metal	0.2715	Experiment
$[Ir_4(CO)_{12}]$	0.2693	XRD
$[Ir_4(CO)_{12}]$	0.269	EXAFS
$[Ir_4(CO)_{12}]$	0.2694	DFT
Ir_4/zeolite NaX	0.270	EXAFS
Ir_4/zeolite NaX	0.271	EXAFS
Ir_4/zeolite NaX	0.25	DFT
Free Ir_4C[b]	0.271	DFT

[a] Notation: DFT, density functional theory; XRD, X-ray diffraction crystallography; EXAFS, extended X-ray absorption fine structure spectroscopy.
[b] C at three-fold hollow site.

Pt might be a favored metal for investigation of ligand effects in clusters, but the samples are not optimal as there are not yet convincing results demonstrating the formation of nearly monodisperse Pt clusters on supports; those nearly uniform clusters that may have been formed (e.g. Pt_{15} [44,45]) are too large for accurate structural characterization by EXAFS spectroscopy. Clusters of other metals, such as Rh_6, may offer better prospects than Pt clusters.

9. Reactivity

Decarbonylation of supported metal carbonyl clusters on hydroxylated supports gives products including CO and CO_2, consistent with chemistry that could break C–C bonds and leave ligands such as C or H on the decarbonylated clusters [46]. By occupying bonding sites on clusters, these ligands would affect adsorption and reaction of other ligands, for example, in catalysis. Work is needed to determine the decarbonylation chemistry and the identities and amounts of any ligands remaining after decarbonylation.

Small supported Pt particles react with O_2; under some conditions, only chemisorption occurs [47]; under other conditions, complete cluster oxidation occurs [43,48]. The chemistry of oxidation of MgO-supported Ir_4 is especially simple [49]: the clusters are fully and reversibly oxidized; the oxidized species are presumably site-isolated iridium oxide clusters.

Supported metal clusters also react with H_2. Reports of the number of adsorbed H atoms per Ir atom of the clusters indicate values <1 [50]. Work is needed to clarify the chemisorption stoichiometries and how they depend on the metal, support and cluster size. The reported data were possibly influenced by effects such as blocking of adsorption sites by ligands such as C or by the support [5,26,50].

Reactions of supported metal clusters with CO give structures that typically do not have the same infrared fingerprints as the metal carbonyl cluster precursors. Thus, the decarbonylation of supported Ir clusters, for example, does not generally appear to be reversible. However, under some conditions, reversibility has been demonstrated. Beutel et al. [51] formed $[Ir_6(CO)_{16}]$ in zeolite NaY, decarbonylated it and cooled it to liquid-nitrogen temperature. Then they brought CO at a pressure of a few mbar in contact with the sample and recorded infrared spectra as the sample was slowly warmed. Initially, the spectrum resembled that of CO adsorbed on highly dispersed Ir on γ-Al_2O_3 [52], but at higher temperatures, the spectra indicated the formation of mononuclear iridium carbonyls, consistent with oxidative fragmentation of the clusters [53], and at a still higher temperature, $[Ir_6(CO)_{16}]$ formed again. This result illustrates fragmentation and cluster reassembly and suggests a method for redispersion of aggregated metal on a support.

Metal clusters on supports, in contrast to those in solution, can be prepared with controlled numbers of ligands, as the coordinatively unsaturated clusters are stabilized by site isolation [54]. Density functional theory was used to investigate the effect of single CO ligands on Ir_4 clusters anchored at the six-rings in zeolite NaX [26]. The results indicate that although the supported clusters bear no charge or a small negative charge (about 0.5 a.u. per Ir_4), the support does cause a polarization of the clusters, indicated by a calculated frequency shift of a CO ligand bonded to the Ir atom farthest from the support [26]. This result is potentially significant for adsorption and catalysis, suggesting how support effects may be understood as ligand effects and ultimately predicted.

Reactions of Ir_4 with propene lead to the formation of propylidyne ligands, identified by their infrared and ^{13}C NMR spectra [55]. These appear to be analogous to propylidyne ligands on (1 1 1) surfaces of metals such as Pt. Further investigation of such ligands on supported metal clusters and comparisons with those on gas-phase clusters and metal single crystals should help to clarify the role of the support.

10. Catalysis

EXAFS spectra representing Ir_4/γ-Al_2O_3, Ir_6/γ-Al_2O_3 and Ir_4/MgO show that the cluster frames were maintained before, during and after catalysis of propene hydrogenation, provided that the conditions were mild (e.g. room temperature and 1 atm) [56] (but when the temperature of catalysis reached about 333 K, the metals aggregated on the support). The data suggest that the supported clusters themselves are catalytically active. The ligands on the clusters during catalysis are not yet determined, and it is possible that residual ligands (such as C) remaining

from the CO of the precursor clusters were present in addition to hydrocarbon and hydrogen.

The rates of toluene hydrogenation catalyzed by Ir_4 and by Ir_6 supported on metal oxides and zeolites differ from each other typically by factors of several; thus, these supports are roughly equivalent, possibly because they all offer similar ligands to the metal cluster [57].

In prospect, structurally well-defined supported metal clusters provide the opportunity for resolving support from cluster-size effects. A family of supported Ir clusters and particles was prepared from $[Ir_4(CO)_{12}]$ on γ-Al_2O_3 [58]. The smallest clusters were approximately Ir_4, and samples with larger clusters and particles was prepared by treating Ir_4/γ-Al_2O_3 in H_2 under various conditions to cause aggregation and vary the average cluster or particle size. The catalytic activity was measured for each sample (Fig. 9). The rate per exposed Ir atom increased by two orders of magnitude as the cluster/particle size increased, becoming independent of particle size when the average particle contained about 100 atoms [58]. The data for the larger particles conform to the expected pattern for the structure-insensitive reaction,

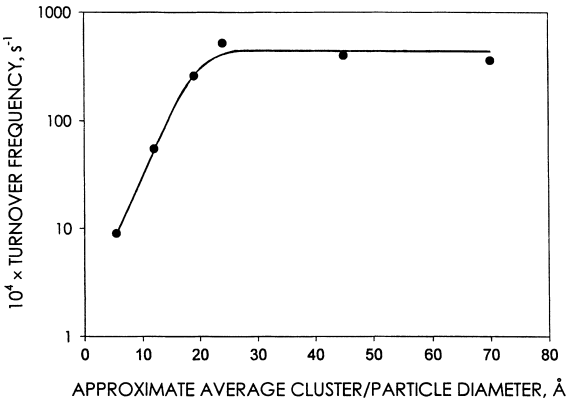

Fig. 9. Dependence of turnover frequency for toluene hydrogenation at 333 K on average iridium cluster or particle diameter [58]. Turnover frequencies were estimated as follows: all the Ir atoms in Ir_4/γ-Al_2O_3 (characterized by EXAFS spectroscopy) were assumed to be accessible in the calculation of turnover frequency; the number of accessible Ir atoms in each of the other catalysts (formed by aggregation of the Ir) was determined by hydrogen chemisorption with an assumed H:Ir ratio of 1:1; clusters and particles other than Ir_4 were assumed to be hemispherical, with the base in contact with the support and inaccessible to reactants.

but those for the smaller clusters and particles do not.

The cluster size dependence is not yet explained; it may reflect an intrinsically low activity of the clusters, but it might also be a consequence of increasing removal of residual ligands such as C from the clusters with increasing severity of treatment in H_2. Other possibilities include a steric effect of the support, limiting adsorption of the reactants on the metal — such an effect would be greatest for the smallest clusters. Nor should an electronic effect be ruled out [12].

11. Opportunities

Supported clusters of only a few metal atoms are new and only partially understood catalytic materials. They offer the prospects of new properties, for example, selectivities. They are the metal catalysts influenced most by supports, and it might be possible to tune their properties by variation of the support and/or the cluster size. These catalysts demonstrate conceptual links between molecular and surface catalysis and contribute to the blurring of these subdisciplines. The fact that they are so simple structurally indicates that increasingly incisive experimental investigations and increasingly rigorous theoretical representations will lead to better understanding of the effects of the metal, support and cluster size. These catalysts seem to be near optimal for such investigations. The emerging results bear out the insights of Boudart's 1985 review [1].

Acknowledgements

Thanks to Michel Boudart for many stimulating discussions. This work was supported by the National Science Foundation (Grant CTS-9615257 and GOALI Grant CTS-9529455), the Department of Energy, Office of Energy Research, Office of Basic Energy Sciences, and a gift from Ford Motor Co.

References

[1] M. Boudart, J. Mol. Catal. 30 (1985) 27.
[2] M. Boudart, Adv. Catal. 20 (1969) 153.

[3] E.L. Muetterties, Bull. Soc. Chim. Belg. 84 (1975) 959.
[4] M. Boudart, G. Djéga-Mariadassou, Kinetics of Heterogeneous Catalytic Reactions, Princeton University Press, Princeton, NJ, 1984 (Chapter 6).
[5] L. Spenadel, M. Boudart, J. Phys. Chem. 64 (1960) 204.
[6] P.D. Nellist, S.J. Pennycook, Science 274 (1996) 413.
[7] J.T. Miller, N.G.B. Agrawal, G.S. Lane, F.S. Modica, J. Catal. 163 (1996) 106.
[8] R.E. Jentoft, M. Tsapatsis, M.E. Davis, B.C. Gates, J. Catal. 179 (1998) 565.
[9] W. Eberhardt, P. Fayet, D. Cox, A. Kaldor, R. Sherwood, D. Sondericker, Phys. Scr. 41 (1990) 892.
[10] H.V. Roy, P. Fayet, F. Patthey, W.-D. Schneider, B. Delly, C. Massobrio, Phys. Rev. B 49 (1994) 5611.
[11] U. Heiz, W.-D. Schneider, in: K.-H. Meiwes-Broer (Ed.), Metal Clusters and Dots, Springer, Heidelberg, 1999.
[12] U. Heiz, A. Sanchez, S. Abbet, W.-D. Schneider, J. Am. Chem. Soc. 121 (1999) 3214.
[13] W.A. Weber, B.A. Phillips, B.C. Gates, Chem. Eur. J. 5 (1999) 2899.
[14] G.A. Panjabi, S.N. Salvi, B.A. Phillips, L.F. Allard, B.C. Gates, to be published.
[15] O. Alexeev, B.C. Gates, J. Catal. 176 (1998) 310.
[16] M. Ichikawa, Adv. Catal. 38 (1992) 283.
[17] S. Kawi, B.C. Gates, in: G. Schmid (Ed.), Clusters and Colloids — from Theory to Applications, VCH, Weinheim, 1994, pp. 299–372.
[18] S. Kawi, B.C. Gates, Inorg. Chem. 31 (1992) 2939.
[19] E.R. Corey, L.F. Dahl, W. Beck, J. Am. Chem. Soc. 85 (1963) 1202.
[20] L.-F. Rao, A. Fukuoka, N. Kosugi, H. Kuroda, M. Ichikawa, J. Phys. Chem. 94 (1990) 5317.
[21] W.A. Weber, B.C. Gates, J. Phys. Chem. 101 (1997) 10423.
[22] K. Asakura, K.K. Bando, Y. Iwasawa, H. Arakawa, K. Isobe, J. Am. Chem. Soc. 112 (1990) 9096.
[23] O. Alexeev, B.C. Gates, Top. Catal. 10 (2000) 273.
[24] B.C. Gates, Chem. Rev. 95 (1995) 511.
[25] B.C. Gates, in: R.D. Adams, F.A. Cotton (Eds.), Catalysis by Di- and Polynuclear Metal Cluster Complexes, Wiley-VCH, Weinheim, 1998, p. 509.
[26] A.M. Ferrari, K.M. Neyman, M. Mayer, M. Staufer, B.C. Gates, N. Rösch, J. Phys. Chem. B 103 (1999) 5311.
[27] J.F. Goellner, K.M. Neyman, M. Mayer, F. Nörtemann, B.C. Gates, N. Rösch, Langmuir, 6 (2000) 2736.
[28] D.C. Koningsberger, B.C. Gates, Catal. Lett. 14 (1992) 271.
[29] N.D. Triantafillou, S.K. Purnell, C.J. Papile, J.-R. Chang, B.C. Gates, Langmuir 10 (1994) 4077.
[30] C.J. Papile, B.C. Gates, Langmuir 8 (1992) 74.
[31] P.S. Kirlin, F.A. DeThomas, J.W. Bailey, H.S. Gold, C. Dybowski, B.C. Gates, J. Phys. Chem. 90 (1986) 4882.
[32] P.S. Kirlin, H. Knözinger, B.C. Gates, J. Phys. Chem. 94 (1990) 8451.
[33] S.K. Purnell, X. Xu, D.W. Goodman, B.C. Gates, Langmuir 10 (1994) 3057.
[34] A. Hu, K.M. Neyman, M. Staufer, T. Belling, B.C. Gates, N. Rösch, J. Am. Chem. Soc. 121 (1999) 4522.
[35] M.G. Samant, M. Boudart, J. Phys. Chem. 95 (1991) 4070.
[36] A. Labouriau, G. Panjabi, B. Enderle, T. Pietrass, B.C. Gates, W.L. Earl, J. Am. Chem. Soc. 121 (1999) 7674.
[37] S. Kawi, O. Alexeev, M. Shelef, B.C. Gates, J. Phys. Chem. 99 (1995) 6926.
[38] A.S. Fung, M.J. Kelley, D.C. Koningsberger, B.C. Gates, J. Am. Chem. Soc. 119 (1997) 5877.
[39] O. Alexeev, S. Kawi, M. Shelef, B.C. Gates, J. Phys. Chem. 100 (1996) 253.
[40] O. Alexeev, M. Shelef, B.C. Gates, J. Catal. 164 (1996) 1.
[41] O. Alexeev, G.W. Graham, M. Shelef, B.C. Gates, J. Catal. 190 (2000) 157.
[42] D.S. Shephard, T. Maschmeyer, G. Sankar, J.M. Thomas, D. Ozkaya, B.F.G. Johnson, R. Raja, R.D. Oldroyd, R.G. Bell, Chem. Eur. J. 4 (1998) 1214.
[43] O.S. Alexeev, B.C. Gates, in: Proceedings of the Twelfth International Congress on Catalysis, 130A (201) 371.
[44] J.-R. Chang, D.C. Koningsberger, B.C. Gates, J. Am. Chem. Soc. 114 (1992) 6460.
[45] T. Yamamoto, T. Shido, S. Inagaki, Y. Fukushima, M. Ichikawa, J. Phys. Chem. B 102 (1998) 3866.
[46] A.K. Smith, A. Theolier, J.-M. Basset, R. Ugo, D. Commereuc, Y. Chauvin, J. Am. Chem. Soc. 100 (1978) 2590.
[47] R.S. Weber, M. Boudart, P. Gallezot, in: J. Bourdon (Ed.), Growth and Properties of Metal Clusters, Elsevier, Amsterdam, 1980, p. 415.
[48] C.-P. Hwang, C.-T. Yeh, J. Mol. Catal. A 112 (1996) 295.
[49] S.E. Deutsch, J.T. Miller, K. Tomishige, Y. Iwasawa, W.A. Weber, B.C. Gates, J. Phys. Chem. 100 (1996) 13408.
[50] O. Alexeev, B.C. Gates, J. Catal. 176 (1998) 310.
[51] T. Beutel, S. Kawi, S.K. Purnell, H. Knözinger, B.C. Gates, J. Phys. Chem. 97 (1993) 7284.
[52] G.B. McVicker, R.T.K. Baker, R.L. Garten, E.L. Kugler, J. Catal. 65 (1980) 207.
[53] H.H. Lamb, B.C. Gates, H. Knözinger, Angew. Chem., Int. Ed. Engl. 27 (1988) 1127.
[54] O. Alexeev, G. Panjabi, B.C. Gates, J. Catal. 173 (1998) 196.
[55] A.M. Argo, B.C. Gates, to be published.
[56] G. Panjabi, A.M. Argo, B.C. Gates, Chem. Eur. J. 5 (1999) 2417.
[57] Z. Xu, F.-S. Xiao, S.K. Purnell, O. Alexeev, S. Kawi, S.E. Deutsch, B.C. Gates, Nature (London) 372 (1994) 346.
[58] F.-S. Xiao, W.A. Weber, O. Alexeev, B.C. Gates, in: Proceedings of the Eleventh International Congress on Catalysis, Part B, Vol. 1135, 1996.